Flexible subwavelength gratings fabricated by reversal soft UV nanoimprint

Liangjin Ge (葛良进)[1], Xudi Wang (王旭迪)[2], Huoyao Chen (陈火耀)[1], Keqiang Qiu (邱克强)[1*], and Shaojun Fu (付绍军)[1]

[1] *National Synchrotron Radiation Laboratory, University of Science and Technology of China, Hefei, 230029, China*

[2] *School of Mechanical and Automotive Engineering, Hefei University of Technology, Hefei 230009, China*

**Corresponding author: blueleaf@ustc.edu.cn*

Received January 13, 2012; accepted March 29, 2012; posted online July 13, 2012

We present a replication process, named reversal soft ultraviolet (UV) nanoimprint, to fabricate a high-aspect-ratio flexible subwavelength grating (SWG) on a polyurethane acrylate (PUA). This nanopatterning technique consists of casting, reversal UV imprint, and dry release. The UV curing process of PUA to avoid pattern collapse is investigated. Revalpha film acts as the supporting and sacrificial layer during the whole process due to its special surface energy property. The free-standing PUA structures with a period of 200 nm and a depth of 350 nm can be automatically released from the Revalpha film by heating. The PUA resist is well suited to replicate fine patterns of the mold with high aspect ratio and large area precisely and uniformly for low surface energy and low viscosity. The measured transmittance is compared with the calculation results based on rigorous coupled-wave analysis in the wavelength region ranging from 500 to 800 nm. The experimental results agree well with the theoretical calculations.

OCIS codes: 050.1950, 050.6624, 220.4241.

doi: 10.3788/COL201210.090502.

Subwavelength gratings (SWGs) with a period smaller than the wavelength of light suppress undesired reflections over a wide spectral bandwidth, similar to an antireflection (AR) surface. AR is widely used to reduce insertion losses at the interfaces between different optical media[1,2]. Optical devices such as solar cells, polarizer light-emitting diodes, and photodetectors integrate SWGs as components[3,4]. To introduce the effective refractive index gradient required for AR applications, subwavelength-structured patterns with tapered profiles and high aspect ratios are highly desirable. These patterns are of interest for many applications, including drug delivery and immunoassay chips. Future flexible electronics and optoelectronics call for the use of flexible substrates. Polymer devices are inexpensive and disposable, thereby being highly desirable for cost-effective applications[5−7].

In recent years, nanoimprint lithography (NIL) has become as a promising technique for forming polymer patterns by pressing a mold into a polymer layer because of its high throughput and low cost. Using conventional NIL, two-dimensional SWGs have been fabricated successfully on polymer (PMMA or polycarbonate, aspect ratio<1). High-aspect-ratio gratings have also been fabricated in SU-8 and PMMA on hard substrates using nanoimprint and casting[8−10]. However, some challenges remain in achieving highly replicated patterns. A release agency is usually necessary to decrease the surface energy of the mold, thereby complicating the process. Higher temperature, bilayer resist process, and higher imprint pressure are needed to make the melt resist fill the trench completely. During the demolding step, the mold breaks, resulting in resist pattern collapse and release failure for the large contact area between the interface of the mold and polymer. In addition, a wet etching process should be used to release the hard substrate from patterned polymer to obtain free-standing structures. However, such processes are time-consuming. Free-standing, flexible high-aspect-ratio structures can be used widely, such as for covering curved surfaces or other components in devices.

In this letter, we present a novel method that uses reversal soft nanoimprinting and enables fabrication of flexible polyurethane acrylate (PUA) SWGs with high aspect ratio (aspect ratio>3), high density, and high resolution in the visible wavelength. The advantages of PUA material are high resolution, low cost, and, most importantly, optical transparency in the visible wavelength. This method overcomes the difficulties and limits of soft lithography and hard-mold-based imprint lithography, such as collapse and release failure due to high modulus and low surface energy of the cured PUA resist. In this replication technique, a multi-step nanopatterning process that includes casting, reversal ultraviolet (UV) imprint, and dry release is developed to achieve the free-standing PUA grating structures. The release agency and wet etching process are not necessary in our method. First, rigorous coupled-wave analysis (RCWA) was used to optimize the parameters of the gratings. Then, the reflectivity for wavelengths ranging from 500 to 800 nm in the visible region was measured.

To calculate the parameters of SWGs, the RCWA method was used to evaluate the transmittance. Figure 1 shows the calculated results of the binary SWGs shown on the right of Fig. 1(a) for several grating depths (D) as a function of incident wavelength. The materials of the grating were assumed to be PUA as well. The PUA film shows good optical properties, such as high transmission (the absorption of the residual layer H was neglected) and a high refractive index compared to PDMS (n=1.4) in the visible region. A higher refractive index increases the diffraction efficiency and minimizes the zero-order

 © 2012 Chinese Optics Letters

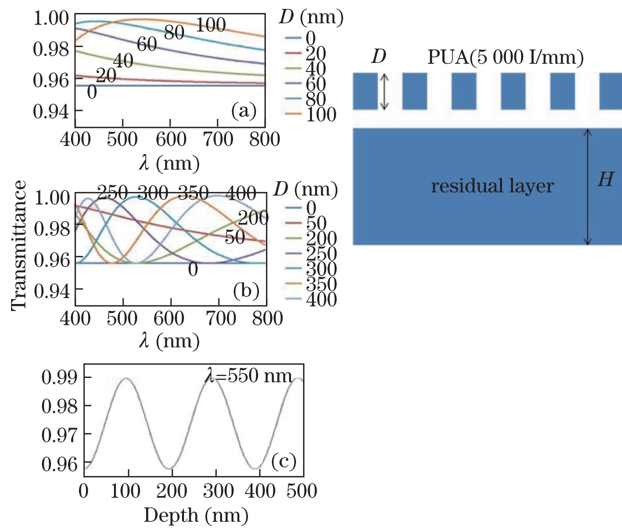

Fig. 1. (Color online) (a) and (b) Calculated transmittance of the binary SWGs for several grating depths as a function of incident wavelength; (c) transmittance as a function of the depth when the incident wavelength is 550 nm.

transmission[11]. In the calculation, the grating period is 200 nm and the line width is 100 nm. The refraction index of PUA is 1.577, compared to the air (n=1.0), which is assumed as the surroundings. As shown in Fig. 1(a), with the increase of the grating depth from 0 nm to 100 nm, the transmittance also increased for wavelengths ranging from 500 to 800 nm. For fixed depth of the grating, the transmittance decreases with the increasing of the wavelength for visible wavelength region as the reflection approaches the solution for the air–substrate interface. Notably, the transmittance becomes flat once the depth is zero without considering the dispersion of the refractive index[12]. With the increase of the depth (d >100 nm), the peak of the transmittance shifts (Fig. 1(b)). Compared to the transmittance 95.5% of the flat surface at the wavelength of 550 nm, the transmittance of the SWG with 300 nm depth gains 3.5% (reaches 99%). With the increase of wavelength, the value increases to the peak, after which it changes cyclically. To realize the periodicity, transmittance as a function of the depth is calculated (Fig. 1(c)). The result shows that the transmittance changes periodically with the increase of the depth. The sine shape clearly explains the shifts of the peak in Fig. 1(b). In the calculation, the incident wavelength is 550 nm and the period is close to 200 nm.

As a main step for the process, mold fabrication was carried out by interference lithography and deep reactive ion etching (DRIE) technique. First, the periodic line patterns (200-nm period and 100-nm linewidth) were obtained in the photoresist layer of 250-nm thickness spin-coated on a silicon substrate. The principle of laser interference lithography is the exposure over the photoresist (PR) by double-beam interference system. The laser used was a He-Cd laser (k=235 nm). By adjusting the incident angle of the double beams, varied periods of the patterns were fabricated. Next, using the patterned resist as an etch mask, we fabricated the Si gratings by using a $C_4F_8/SF_6/O_2$ gas mixture DRIE, followed by removal of the residual resist using acetone and IPA to achieve clean and vertical side walls. In this etching process, O radicals can prevent the recombination reaction of SF_6 plasma and increase the F-atom density when O_2 gas of an appropriate amount is added to the C_4F_8/SF_6. In addition, $Si_xO_yF_z$ film could be generated on the side wall and act as passivation due to O radicals, thereby initially increasing selectivity by adding oxygen. We should note that the sharp trench profile and etch selectivity will drop with further increase of oxygen flow rate.

Grating patterns of 200 nm are merely a subwavelength range for UV-visible light, which is the basis of our process design. In this reversal soft UV imprint technology, a silicon mold without modified surface was spin-coated with an UV-curable polymer, then transferred onto a flexible substrate during an UV imprint process. This process was followed by the peeling-off step. High-end facilities are not necessary to make uniform pattern transfer of the size of stamps. Figure 2 illustrates how our process works. First, UV-curable polymer PUA was spin coated or poured onto an etched silicon mold to obtain various thickness of the PUA monomer, which was then brought into contact with a flexible supporting layer. For some special uses such as curved surface, the SWG structure needs to be incumbent on another structure or bonded with other substrate; however, it has to be separable. In order to achieve this goal, in this experiment, Revalpha sheet, a dry adhesive film from Nitto Denko Co., was used as the supporting layer because of its property of releasing automatically when heated at 120 °C. Moderate pressure was applied to induce slight polymer wetting for adhesion to the Revalpha sheet. After a couple of minutes, UV-light radiation was supplied through the supporting layer to the PUA layer. PUA monomers undergo cross-linking under UV exposure to form a hard epoxy material. Afterwards, the silicon mold was removed, and the molded PUA structures were left on the Revalpha sheet. Finally, the free-standing PUA structures could be automatically released from the Revalpha film by heating at a temperature of 120 °C.

Figure 3(a) shows the scanning electron microscope (SEM) photograph of the silicon mold obtained in the experiment section, with rectangular grooves, 200-nm period and 350-nm depth SWG from the measurement result. In the DRIE process, the Si side walls were coated with passivation polymer from C_4F_8 dissociation, whereas the bottom of the exposed trenches was etched by ion bombardment. The side wall verticality could be well controlled by the added oxygen gas. The replicated SWGs on the PUA resist are shown in Figs. 3(b) and 3(c). The exact period (200 nm), duty cycle (1:1), and depth (350 nm on average) demonstrate a successful and

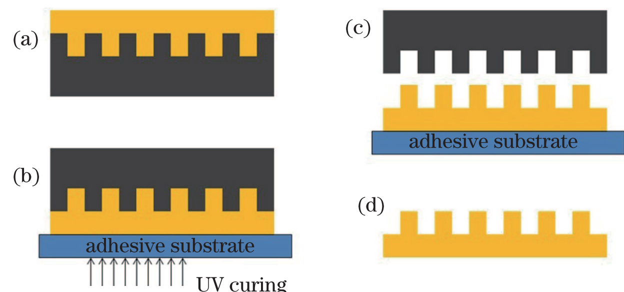

Fig. 2. Diagram of the process flow for PUA SWG fabrication.

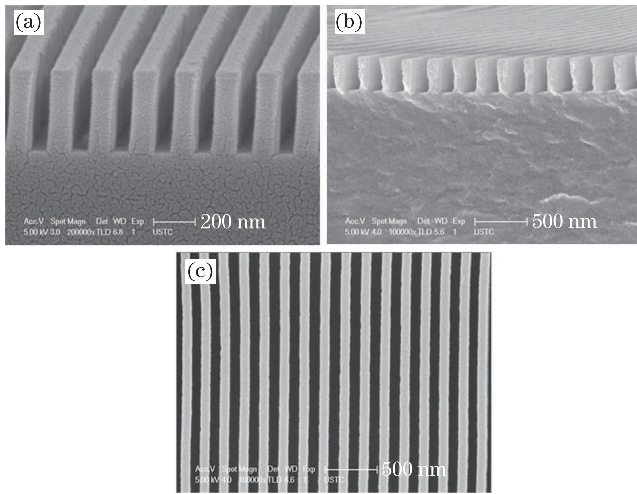

Fig. 3. SEM photographs of (a) Si mold and the (b) cross-sectional view and (c) top view of replicated PUA SWG.

precise replication from the mold. The top and cross-section views show the excellent replication property of PUA. At room temperature, large-area PUA patterns (1×1 (cm)) can be replicated uniformly with high resolution and high precision because of the low viscosity of the uncured PUA. The absence of breakings and air bubbles in both molds and PUA patterns after ten experiments shows the good repetitiveness of the process. Routine application of a release agent to the templates for easy demolding was not necessary to our work due to the low surface energy of cured PUA. Because no pressure was applied during the casting process, the etched Si masters sustained no damage, even after numerous replications. Even if some residue (i.e., a clogged hole, uncured monomer) remained after the replication process, thermal or chemical removal of the residue would not degrade the master.

High-aspect-ratio nanopillar arrays can collapse under their own weight (ground collapse) or through adhesion to one another (lateral collapse) when adhesive force or capillary force is sufficiently high to cause contact between them[13]. Using the lateral collapse theory established by Hui, Junyong Park et al. discovered that cured PUA has a sufficiently high rigidity (≈1.7 GPa), greater than E_c^*[11], which theoretically means no lateral collapse. However, during our experiments, collapse caused by the low rigidity still occurred when the curing dose was not sufficient to cure the PUA completely, as shown in Fig. 4. Every two or more nanogratings adhered to each other to form bundles and the pattern lost initial grating color. With the increase in UV curing time, the flexibility of the PUA monomer decreased only slightly. To confirm the effect of the curing time precisely, we used Fourier transform infrared spectroscopy to test the sample, and found that the C=C double bond in PUA decreased obviously with the curing time in the first 20 min. After 20 min, the C=C double bond decreased very slowly, which meaned the best choice of the curing time is 20 min. Actually, when the UV curing time is over 10 min, the PUA monomer shows sufficiently high hardness and good flexibility to avoid the collapse issues.

For the complete transfer of PUA structures from the silicon mold, the control of mold surface energy is important. Polymer coating requires the mold surface energy to be sufficiently high to ensure good adhesion of the polymer to the mold surface. Primarily, the pattern precision during the transfer is dependent on the PUA being completely filled. The uncured PUA has low viscosity, and its contact angle between PUA and Si mold is sufficiently small to be filled completely. Furthermore, during the release process, mold surface energy needs to be lower than that of the substrate so that the PUA will adhere more strongly to the substrate than to the mold. Therefore, the mold surface energy must be tailored to satisfy these requirements. After curing, the surface energy of PUA (≈25 dyne cm^{-1}) used here[14] decreased dramatically and became smaller than that of the Revalpha sheet; thus, transferring the PUA onto the flexible substrate was easy. PET film could also be used as the backing layer instead of Revalpha sheet. For the complete transfer of the PUA structures, PET surface should be pretreated with oxygen plasma for 30 s. However, we could not separate the PUA layer from the PET substrate to obtain the free-standing PUA gratings because the bonding strength between PUA and PET was too high.

Figure 5 shows the transmittance of the replicated SWG as a function of wavelength. In the calculation, the structure was replicated and attached on the PET substrate. The sample was divided into SWG, residual PUA, and PET layer. The theoretical transmittance calculated based on RCWA is shown in Fig. 1(b) (D=350 nm). The transmittance of the PUA residual layer and PET layer was calculated by multi-layered thin-film program[15]. As a result, the calculated transmittance of the flat surface was 95.5% on average. We measured the transmittance, as shown in Fig. 5(a). According to the measured results, a 2% fluctuation range of the transmittance around the central was present because of the difference interference between SWG and flat PUA. As shown in Fig. 5(b), the calculated values can explain the phenomenon well. We can see that the experimental values are equal to the theoretical model in the visible wavelength. The slight error, which may be caused by resist or system loss, is acceptable. Because the PET is sufficiently thick, the theoretical calculation does not consider the interference in PUA and PET.

In conclusion the design and fabrication of antireflection SWGs of free-standing with the 200-nm period and 350-nm depth are both studied based on a reversal soft UV nanoimprint method. PUA shows low surface energy, high modulus, and excellent optical transmittance. We demonstrate that the above

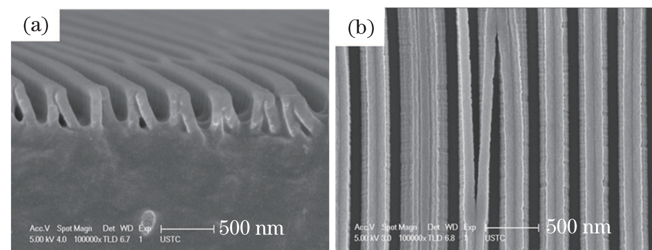

Fig. 4. SEM of the replicated PUA SWG with lateral collapses: (a) cross-sectional and (b) top views.

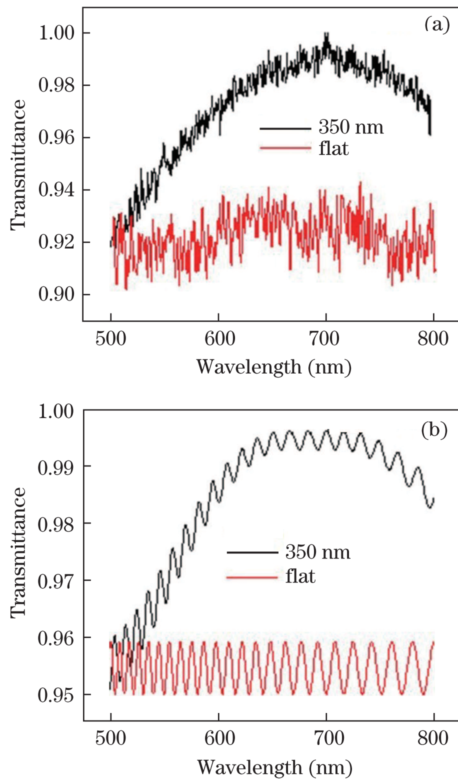

Fig. 5. Transmittance of the replicated SWGs as a function of visible wavelength: (a) experimental and (b) calculated values.

method is a good way to replicate large-area and high-aspect-ratio patterns precisely and uniformly. The curing process of PUA is studied to overcome the collapse problem. We compare the experimental results of the transmittance at wavelength from 500 to 800 nm with the theory analysis based on RCWA, and find the error to be acceptable and the results to be reasonable. The increased transmittance by the SWG is 4% at most.

This work was supported by the National "863" Program of China (No. 2008AA04Z303) and the National Natural Science Foundation of China (No. 11005111).

References

1. Y. Kanamori, E. Roy, and Y. Chen, Microelectron. Eng. **78,** 287 (2005).
2. Z. Yu, H. Gao, W. Wu, H. Ge, and S. Y. Chou, J. Vac. Sci. Technol. B **21,** 2874 (2003).
3. B. Schnabel, E. Kley, and F. Wyrowski, Opt. Eng. **38,** 220 (1999).
4. J. Xu , C. Cheng, Z. Zheng, J. Chen , Q. Bai, C. Liu, and H. Wang, Chin. Opt. Lett. **8,** 807 (2010).
5. S. J. Wilson and M. C. Hutley, Opt. Acta **29,** 993 (1982).
6. Y. Zhang, C. Lo, J. Ashley Taylor, and S. Yang, Langmuir **22,** 8595 (2006).
7. M. Kang and L. J. Guo, J. Vac. Sci. Technol. B **26,** 2421 (2008).
8. X. Wang, Y. Chen, S. Banu, H. Morgan, S. Fu, and Z. Cui, Microelectron. Eng. **84,** 872 (2007).
9. Y. Hirai, T. Konishi, T. Yoshikawa, and S. Yoshida, J. Vac. Sci. Technol. B **22,** 3288 (2004).
10. T. Konishi, H. Kikuta, H. Kawata, and Y. Hirai , Microelectron. Eng. **83,** 869 (2006).
11. J. Park, J. H. Park, E. Kim, C. W. Ahn, H. I. Jang, J. A. Rogers, and S. Jeon, Adv. Mater. **23,** 860 (2011).
12. E. B. Grann, M. G. Moharam, and D. A. Pommet, J. Opt. Soc. Am. A **12,** 333 (1995).
13. H. Schmid and B. Michel, Macromolecules **33,** 3042 (2000).
14. S. J. Choi, P. J. Yoo, S. J. Baek, T. W. Kim, and H. H. Lee, J. Am. Chem. Soc. **126,** 7744 (2004).
15. M. A. Macleod, *Thin-Film Optical Filters* (2nd ed.) (CRC Press, Florida, 1986).